Submitted to the 29th International Conference on High-Energy Physics ICHEP98,
Vancouver, Canada, July 1998

Antideuteron Production at HERA and Search for Heavy Stable Charged Particles

H1 Collaboration

Abstract

A search has been performed for stable heavy charged particles in photoproduction at HERA. The study is based on about $3.5 \cdot 10^6$ selected multi-hadronic events, taken by the H1 detector and corresponding to $8\ \mathrm{pb}^{-1}$ of integrated luminosity. The rate of antideuteron production has been measured. The properties of the events containing antideuterons are investigated. An upper limit is set for the production of charged particles with masses larger than the deuteron mass.

Abstract: 585
Parallel sessions: 10,5
Plenary sessions: 12,7

1 Introduction

The present analysis addresses two main questions. First, a search is performed for new, exotic heavy (mass $M_x > M_p$) charged ($q \geq 1$) and stable (or quasistable with the life time $\tau > 10^{-8}$ sec) particles. This is a traditional task at every high energy accelerator. Here we profit from high statistics which is comparable to or even exceeds that at existing hadron-hadron and e^+e^- colliders.

The second question is antideuteron and possible antitriton production in ep collisions at HERA energies. The mechanisms of those processes, although allowed within the Standard Model, are not fully understood yet. Antideuterons have been found in fixed target proton-nucleus [1] and proton-proton [2] interactions. The ARGUS experiment [3] reported an observation of the antideuterons in the decay modes of the Υ(1s) state in e^+e^- collisions at 10 GeV. The latter case gives a spectacular manifestation of energy to matter transformation. In the OPAL experiment [4] in e^+e^- collisions at higher energy (Z^0 resonance) antideuterons have not been observed. In general, the observation of antideuterons indicates the level of statistics and the ability of the experiment to search for new heavy particles.

2 Experimental Procedure

2.1 The H1 Detector

The H1 detector is described in detail elsewhere [5]. A brief account of the components that are most relevant to the present analysis is given here. These are the positron tagger, the central tracker, the backward calorimeter (Spacal) and the liquid argon (LAr) calorimeter. The direction of the z-axis is chosen to be along the proton beam direction. The polar angle θ is defined with respect to the z-axis and pseudorapidity is given by $\eta = -\ln(\tan\theta/2)$.

The positron tagger, located at $33\,\mathrm{m}$ from the interaction point in the positron beam direction, measures the energy of the scattered positron and, in conjunction with a photon detector, the luminosity by exploiting the Bethe-Heitler process $ep \rightarrow ep\gamma$.

The central track detector consists of an inner and an outer concentric central jet chambers (CJC), multi-wire proportional chambers for triggering purposes and two additional drift chambers which measure accurately the z-coordinate. The pseudorapidity range covered by the central track detector is $|\eta| < 1.5$. The CJC has 56 sensitive wire layers and is filled with a gas mixture of Ar-$Ethane$ $(50\% : 50\%)$ at atmospheric pressure. The track detector is placed inside an uniform magnetic field of 1.15 T. The CJC measures the transverse momentum and the specific energy loss $\mathrm{d}E/\mathrm{d}x$ of the charged particles. The transverse momentum resolution is $\sigma_{p_t}/p_t \approx 0.009 \cdot p_t[GeV] \oplus 0.015$. The typical $\mathrm{d}E/\mathrm{d}x$ resolution is $\sigma(\mathrm{d}E/\mathrm{d}x)/(\mathrm{d}E/\mathrm{d}x) \approx 7.5\%$ for 56 charge samples on a minimum ionizing track.

The LAr and Spacal calorimeters surround the tracking system and cover the angular range $4^\circ < \theta < 154^\circ$ and $153^\circ < \theta < 177.8^\circ$ respectively.

2.2 Data Sample and Event Selection

The measurements presented here are based on the H1 data taken during 1996 and correspond to an integrated luminosity of about 8 pb^{-1}. High statistics minimally biased photoproduction sample is used. Photoproduction events are selected by requiring the presence of a scattered positron in the small angle positron tagger. For these events the photon virtuality is $Q^2 < 10^{-2}$ GeV^2. The energy measured by the positron tagger is used in the determination of the total γp collision energy W. In the main detector γp events are triggered by demanding, in addition to a signal in the positron tagger, the presence of at least three tracks in the CJC.

In order to reduce the non-ep background contamination and to ensure good reconstruction of the event kinematics, the following selection criteria have been applied for this analysis:

- Photoproduction events are required to lie within the interval $150 < W < 260$ GeV. This corresponds to an average photon–proton collision energy of $W = 200$ GeV.
- The trigger conditions are verified by selecting multi-hadronic events with more than two reconstructed tracks pointing to the common event vertex.
- In order to suppress random coincidences between the high rate Bethe-Heitler events and beam-gas background in the main H1 detector, events were rejected if a photon with an energy $E_\gamma > 2\ \mathrm{GeV}$ was detected in the photon tagger.
- The event vertex reconstructed from the tracks of charged particles was required to lie within ± 30 cm of a nominal $z-$position of the interaction point, corresponding to about 3σ cut on the interaction region defined by the longitudinal size of the proton bunch. In the transverse plane the events with $R_{vertex} > 2.5$ cm were removed.

In total about $3.5 \cdot 10^6$ events satisfy the above selection criteria. The selected events contain both the primary particles originating from the common event vertex and secondary particles resulting from rescatterings in the detector volume.

2.3 Charged Particle Identification

The particle identification is based on simultaneous measurement of the momentum p and the specific energy loss $\mathrm{d}E/\mathrm{d}x$, which is performed in a multi-sample system of the CJC. A special treatment is necessary in order to achieve the most accurate determination of $\mathrm{d}E/\mathrm{d}x$ for full track from the set of the partial measurements $(\mathrm{d}E/\mathrm{d}x)_i$. A simple mean value $\langle \mathrm{d}E/\mathrm{d}x \rangle$ is not an adequate estimate, because the Landau distribution has an infinite dispersion. Therefore, most often the truncated method (TRM) is used, first proposed in [6], in which by cutting out the tail of $\mathrm{d}E/\mathrm{d}x$ distribution one makes the new distribution with the finite dispersion. In the H1 experiment another method of $\mathrm{d}E/\mathrm{d}x$ treatment is used, in which by the scale conversion the tail contribution is suppressed. These methods, although being rather efficient, do not make use of all available information. This problem is naturally solved in a Likelihood Method (LHM). The method was first proposed and developed in [7]. Here the main advantages of LHM are briefly outlined.

For a given momentum the particle separation is determined both by the $\mathrm{d}E/\mathrm{d}x$ resolution and the distance between the branches of the $\mathrm{d}E/\mathrm{d}x$ curve for different particles:

$$S_{ab} = \frac{\log(\mathrm{d}E/\mathrm{d}x)_a - \log(\mathrm{d}E/\mathrm{d}x)_b}{\sqrt{\sigma_a^2 + \sigma_b^2}} \tag{1}$$

where a and b are two particle types and $\sigma_{a(b)}$ is a relative $\mathrm{d}E/\mathrm{d}x$ resolution. LHM of $\mathrm{d}E/\mathrm{d}x$ treatment gives better separation power as compared to the traditional TRM approach. The improvement is especially important for heavy, highly ionizing particles. This is because the change in shape of the $\mathrm{d}E/\mathrm{d}x$ distribution within a given interval becomes more pronounced and can no longer be ignored. For example, using H1 central tracker data the following results are obtained for kaon-proton (KP) and proton-deuteron (PD) separation:

$$S_{KP}(LHM) = 5.47, \quad S_{KP}(TRM) = 4.70$$

$$S_{PD}(LHM) = 6.55, \quad S_{PD}(TRM) = 3.87.$$

The observed ionization energy loss in a logarithmic scale, versus a logarithm of the momentum for positively charged tracks with the number of hits $N_{hit} > 40$ is shown in fig. 1. The scatter plot illustrates a rather good resolution of left branches of the ionizing curves for different kinds of particles. As seen from fig. 1, low p/M parts of the ionizing curve for different particles are to a good approximation parallel straight lines:

$$\mathrm{d}E/\mathrm{d}x \propto (M/p)^n \tag{2}$$

It is known, that in the ideal case (Bethe-Bloch equation) the power n is expected to be approximately $5/3$ [8]. In reality however, the effective slope depends on various parameters of the measurement system and even on the analysis method. For the H1 tracker one gets $n \approx 1.3$ using the LHM and $n \approx 1.2$ for TRM.

The relation (2) gives to a good approximation the mass of the particle, M, when $\mathrm{d}E/\mathrm{d}x$ is above a certain threshold. For further analysis we use the cut $\mathrm{d}E/\mathrm{d}x \geq 2 \cdot MIP$ (minimally ionizing particle).

2.4 Background and Track Selection

Fig. 2 shows the mass spectra and the distributions of the distances of closest approach (DCA) to the beam axis in the plane transverse to beam direction, for positive and negative particles. The peaks of kaons, protons and deuterons are clearly resolved in the mass distributions. Although the bulk of the tracks originate from the primary vertex (DCA peak around zero), the background from secondary interactions is not negligible.

For positive tracks, the main source of the background is nuclei fragmentation in a secondary interaction of fast particles with the matter, as the structure of DCA distribution shows (the beam pipe at ~ 4.5 cm radius, the inner wall of the chamber at ~ 20 cm etc.). The negative particle background has flat distribution and much lower rate. It is mainly due to back-scattered protons and deuterons produced in the detector material and hence reconstructed with an opposite sign of the charge (albedo particles). The suppression of such kind of background is done by constraining all tracks to the main event vertex, located in the beam area in space:
$\mid z_{ver} - z_{DCA} \mid < 7$ cm and $\mid DCA \mid < 1$ cm.

In addition, since the background particles have soft momentum spectra, their proportion increases with increasing $\mathrm{d}E/\mathrm{d}x$. This is taken into account by the selection of tracks with $\mathrm{d}E/\mathrm{d}x < 8 \cdot MIP$ and by applying the minimum momentum cut for charged particles, $p > 0.55$ GeV/c.

In order to ensure high efficiency for the track reconstruction and particle identification the tracks for the analysis are selected within the $|\cos(\theta)| < 0.8$ angular interval, which corresponds to the pseudorapidity range $|\eta_{lab}| < 1$.

To achieve best possible $\mathrm{d}E/\mathrm{d}x$ resolution only tracks with large number of hits were selected. To equalize the identification efficiencies for positive and negative tracks which differ because of the Lorentz angle effect and the asymmetry in CJC construction, the cut on the number of hits per track was set at $N_{hit} > 55$ for negative particles and $N_{hit} > 40$ for positive ones. Finally, only fully efficient areas of the 1996 setup of the CJC were used. These areas covered 48% of the full azimuthal angular interval.

In total, an overall track selection, reconstruction and identification efficiency $\epsilon = 0.44 \pm 0.09$ was obtained.

3 Results

The mass spectrum of negatively charged particles in the ionization interval from 2 to 8 MIP is shown in fig. 3. One can see a pronounced signal of antideuterons on top of the antiproton tail.

The scaled momentum distribution of negative particles with a value of $\log_{10} M$ lying within a window of ± 0.1 around the nominal value of the deuteron mass is shown in fig. 4, as compared to the similarly obtained spectra for antiprotons and K^-. The three distributions in fig. 4 (a,b,c) have similar shape, rising with increasing p/M. This is a characteristic feature of particles created in high energy ep interactions. On the contrary, background particles selected from the tails of DCA distribution, such as evaporated baryons and nuclear fragments produced in the material of the detector and faking eventually "antideuterons" by the albedo, have significantly softer distributions and can easily be distinguished, as illustrated by fig. 4 (d).

The high mass tails for both negatively and positively charged particles are shown in fig. 5. To ensure better separation the tracks for these distributions were restricted to the interval $4 < (\mathrm{d}E/\mathrm{d}x)/MIP < 8$, which corresponds to the scaled momentum range $0.30 < p/M < 0.52$. A clear antideuteron peak is seen, which is well separated from the tail of the antiprotons. The number of observed antideuterons $N_{\bar{D}} = 20$. The total amount of misidentified background in this signal was obtained from the tail of the DCA distribution and found to be 0.3 ± 0.2.

Taking into account the overall antideuteron track efficiency, $\varepsilon = 0.44 \pm 0.09$, the rate of antideuteron production per multi-hadronic (MH) event in photoproduction at 200 GeV is determined to be

$$w_{\bar{D}}(0.55 < p_{\bar{D}} < 1.0 \text{ GeV}/c) = \frac{N_{\bar{D}}}{N_{MH} \cdot \varepsilon} = (13 \pm 4) \cdot 10^{-6}.$$

Some other identified particles have been observed in antideuteron events: 2 K^+, 2 K^-, 7 protons and zero antiprotons. The strong excess of the protons accompanying antideuteron events gives additional evidence of the antibaryonic nature of the particles identified here as antideuterons.

It is worth mentioning that the rate of antideuteron production measured in present analysis is similar to those obtained by the ARGUS experiment [3], in spite of significant difference in energy and in the nature of colliding particles.

No stable negative particles with mass $M > 2.4$ GeV/c^2 and no stable positive particles with mass $M > 3.5$ GeV/c^2 are found in the considered momentum range. Hence the upper limit for the probability of new heavy particle production at 90% CL is:

$$w(0.30 < \frac{p}{M_x \cdot q} < 0.52) < 1.5 \cdot 10^{-6}.$$

4 Conclusions

Antideuteron creation is observed in photoproduction at $W = 200$ GeV in the momentum interval $0.55 < p_{\bar{D}} < 1.0$ GeV/c with the rate

$$w_{\bar{D}} = (13 \pm 4) \cdot 10^{-6}.$$

The momentum distribution of $\bar{D}$ rises with increasing momenta. This is a characteristic feature of the particles produced in genuine high energy ep collisions. Strong excess of protons accompanying antideuteron particles confirms the antibaryonic nature of $\bar{D}$.

No stable negative particles with mass $M > 2.4$ GeV/c^2 and no stable positive particles with mass $M > 3.5$ GeV/c^2 are observed. This results in the upper limit:

$$w(0.30 < \frac{p}{M_x \cdot q} < 0.52) < 1.5 \cdot 10^{-6}.$$

for heavy stable particle production in γp collisions at 200 GeV.

5 Acknowledgements

We are grateful to the HERA machine group whose outstanding efforts have made and continue to make this experiment possible. We thank the engineers and technicians for their work constructing and now maintaining the H1 detector, our funding agencies for financial support, the DESY technical staff for continual assistance and the DESY directorate for the hospitality which they extend to the non-DESY members of the collaboration.

References

[1] D.E. Dorfan et al., Phys. Rev. Lett. **14** (1965) 1003;
Y.M. Antipov et al., Phys. Lett. **B29** (1969) 245.

[2] M.G. Albrow et al., Nucl. Phys. **B97** (1975) 189.

[3] ARGUS Collaboration, H. Albrecht et al., Phys. Lett. **B157** (1985) 326;
ARGUS Collaboration, H. Albrecht et al., Phys. Lett. **B236** (1990) 102.

[4] OPAL Collaboration, R. Akers et al., Z. Phys. **C67** (1995) 203.

[5] H1 Collaboration, I.Abt et al., Nucl. Instr. and Meth. **A386** (1997) 310 & 348.

[6] V.A. Lubimov, G.P. Eliseev and V.K. Kosmachevskii, Izvestija AN SSSR (Ser. Phys.) **19** (1955) 753.

[7] A.I. Alikhanov, V.A. Lubimov and G.P. Eliseev, CERN Symposium on High Energy Accelerator and Pion Physics, CERN, Geneva (1956).

[8] Particle Data Group, Phys. Rev. **D54** (1996) 132.

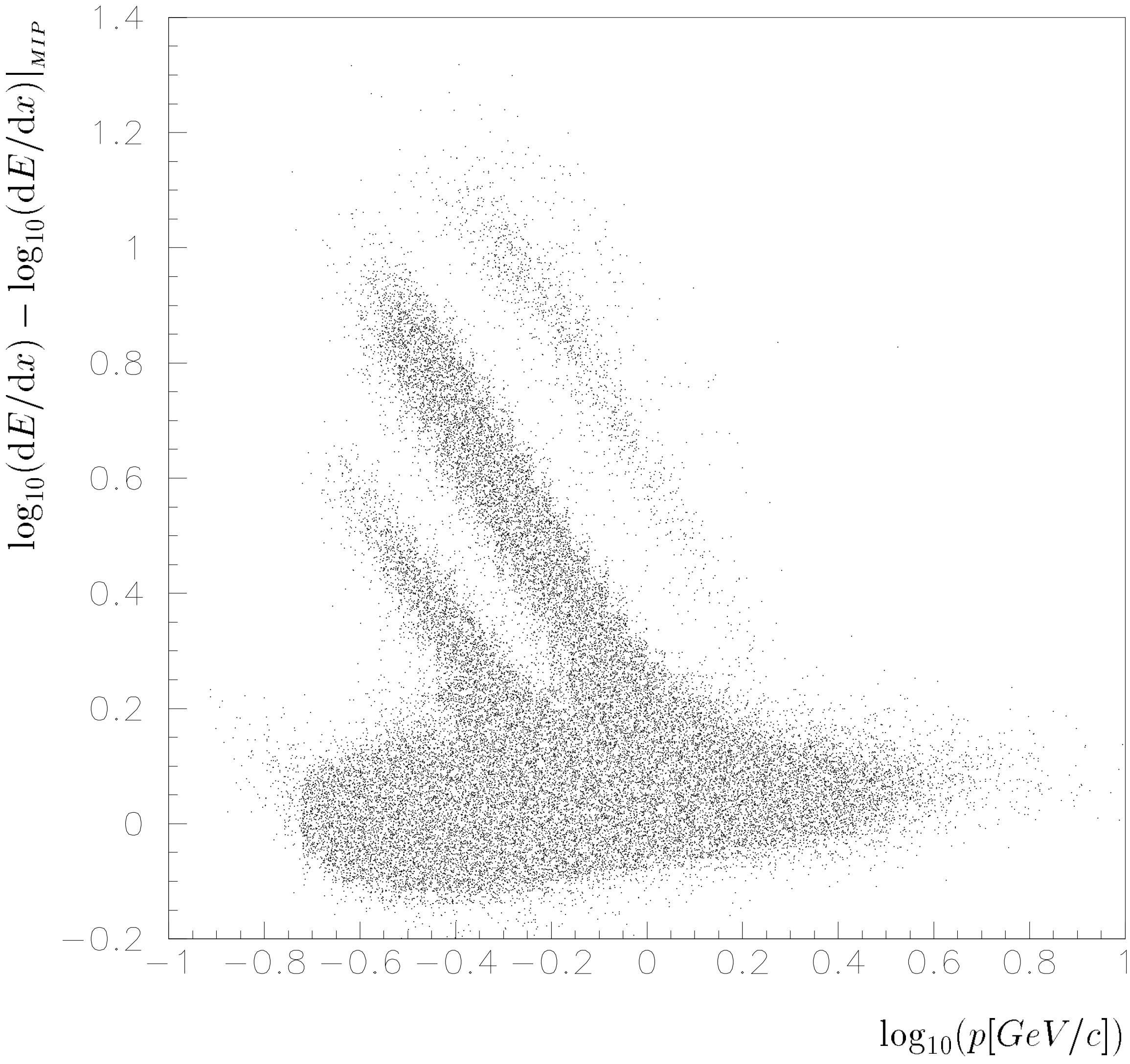

Figure 1: The ionization energy loss as a function of the momentum for positively charged tracks with the number of hits $N_{hit} > 40$.

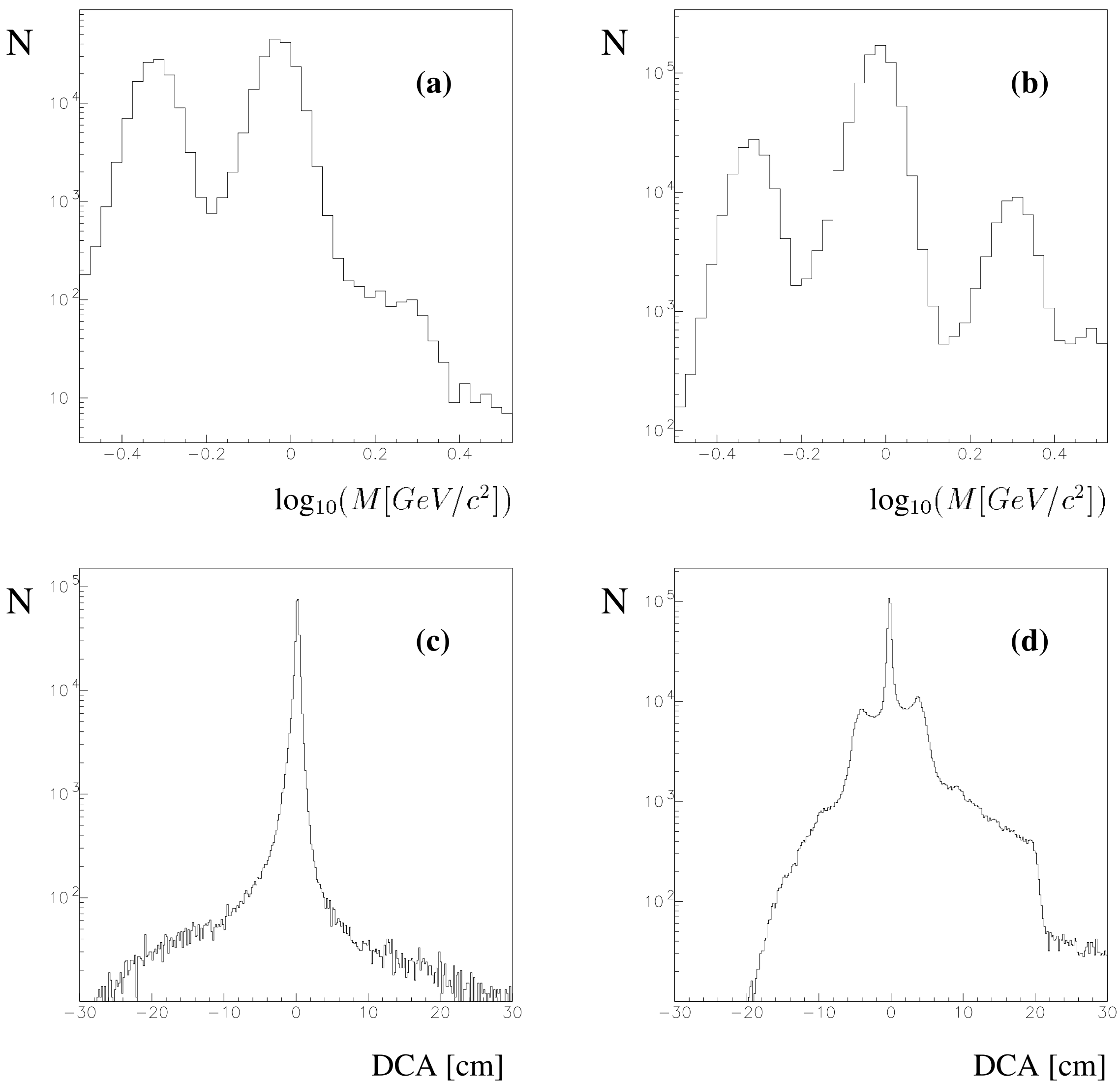

Figure 2: Mass spectra (a,b) and DCA distributions (c,d) for negative (a,c) and positive (b,d) particles.

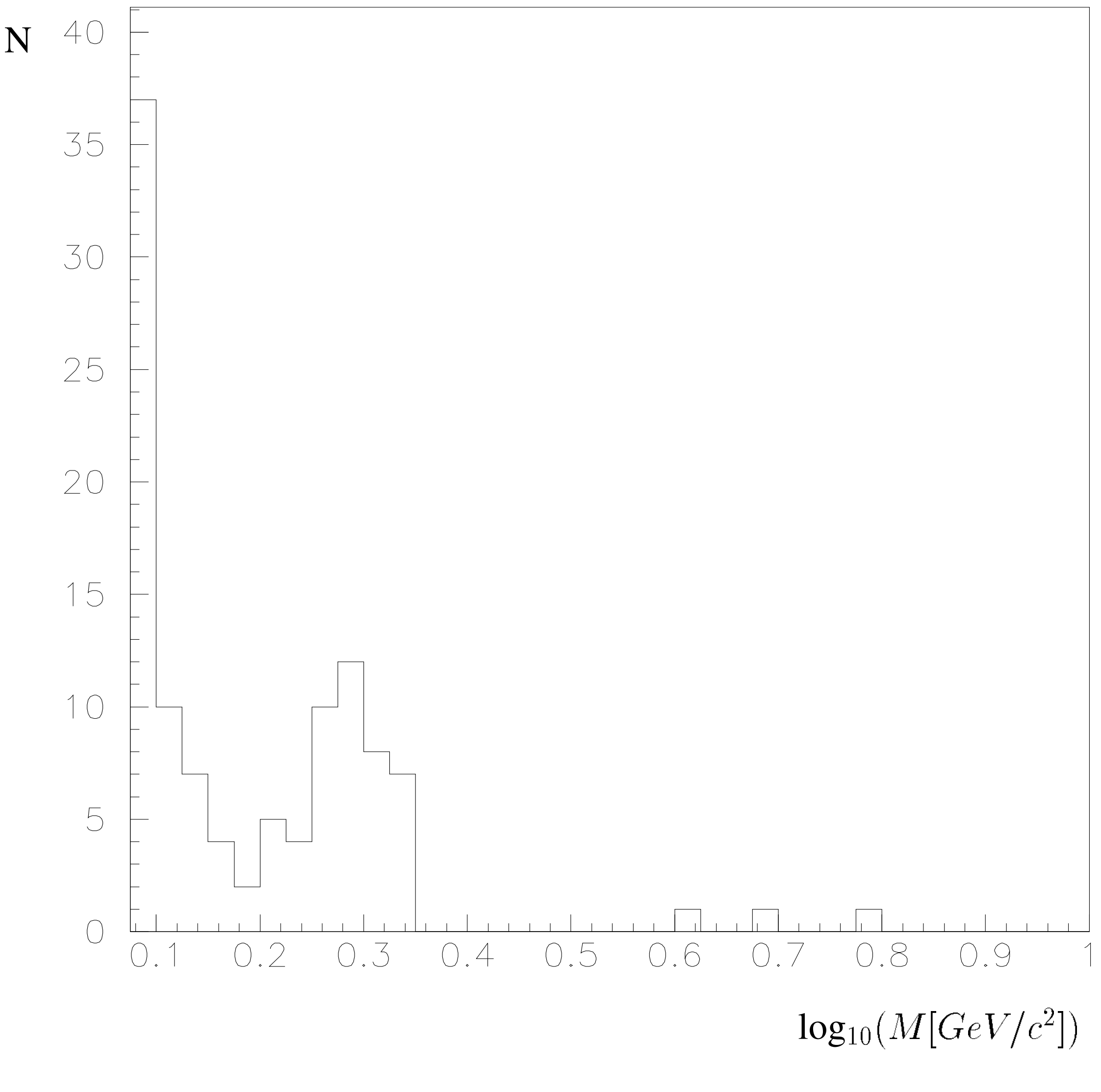

Figure 3: Logarithmic mass spectrum of negative particles measured in the scaled momentum range $0.30 < p/M < 0.90$ and $\mid \eta_{lab} \mid < 1$.

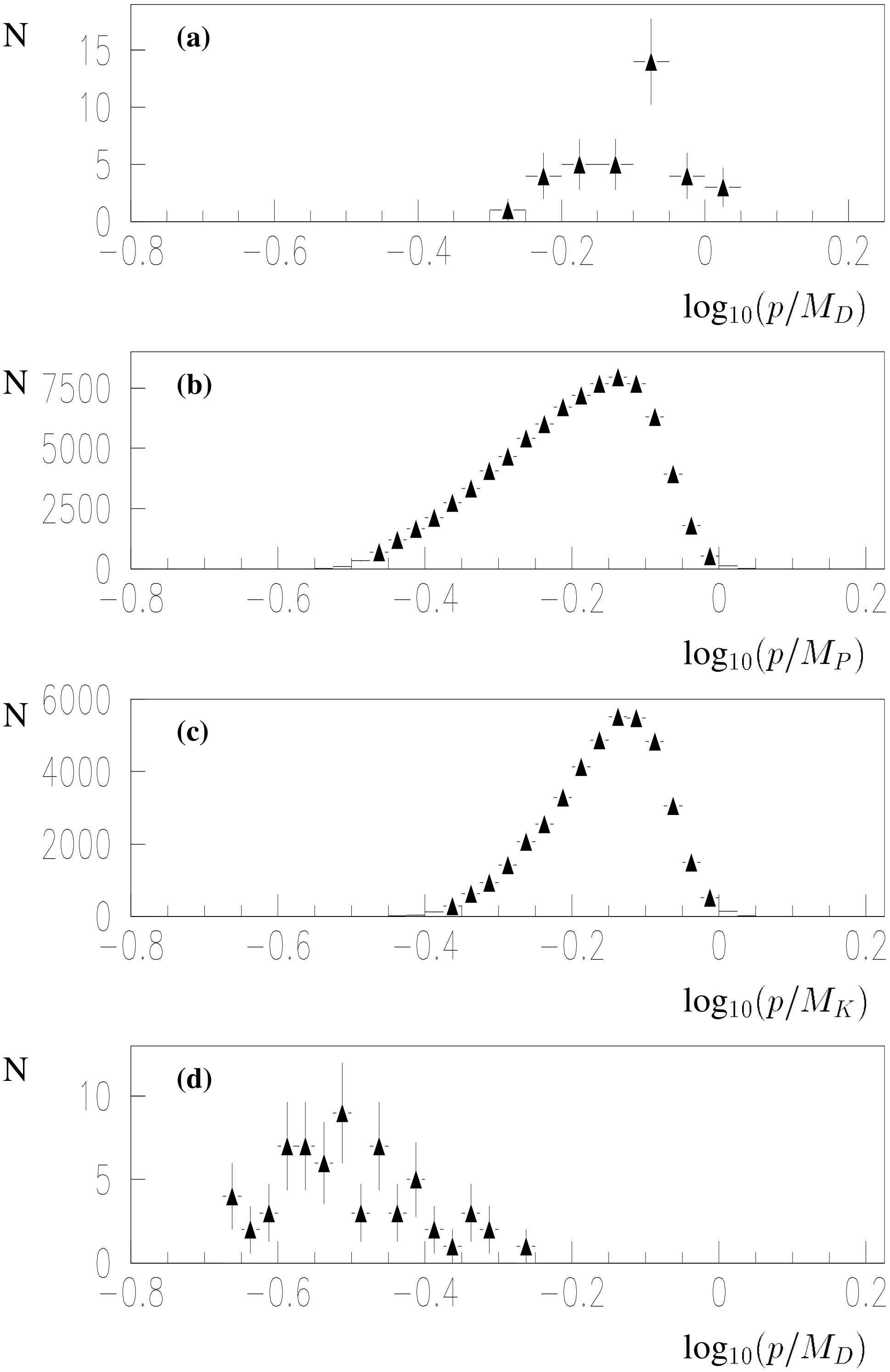

Figure 4: Normalised momentum distribution of identified antideuterons (a) in comparison with antiprotons (b), negative kaons (c) and "antideuteron" background from the albedo (d).

H1 preliminary

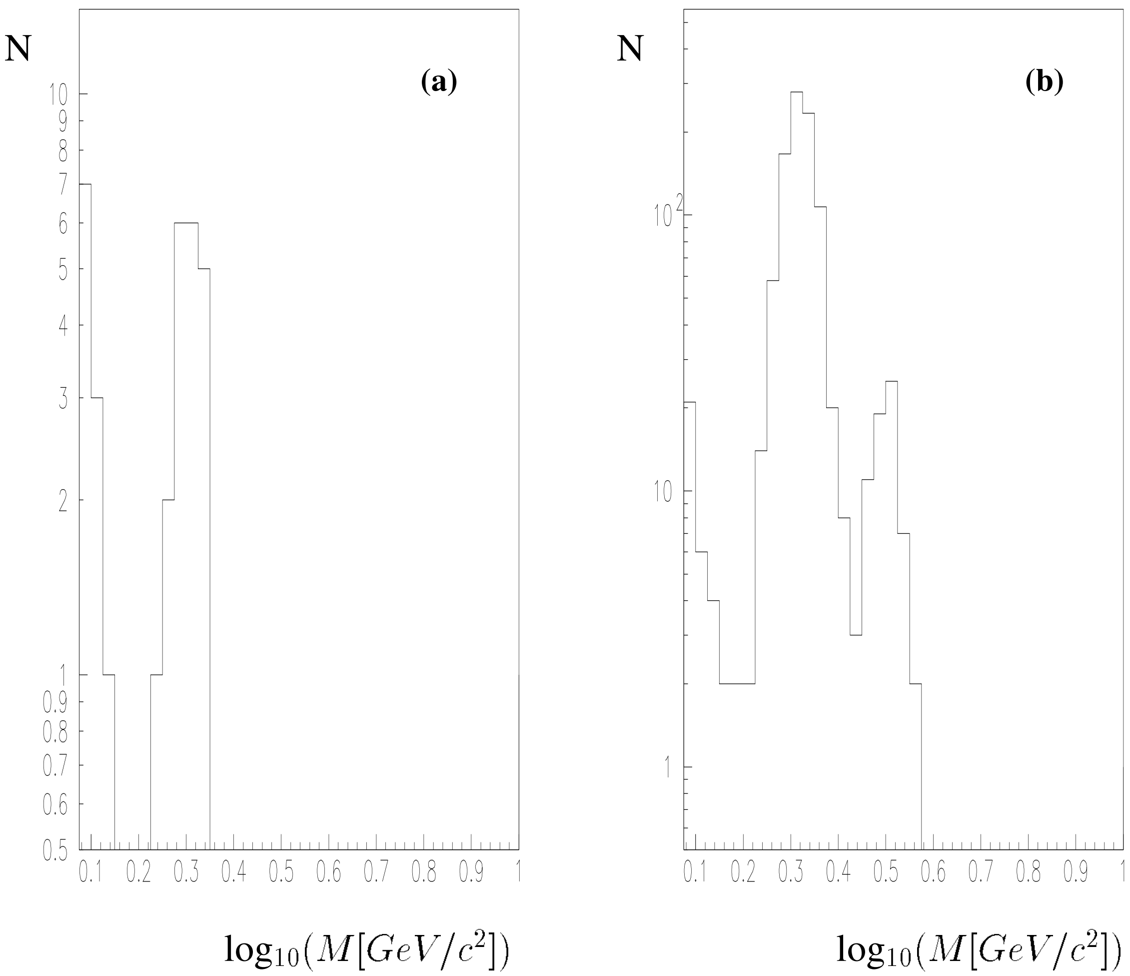

Figure 5: Logarithmic mass distribution for heavy stable negative (a) and positive (b) particles, produced at HERA in the range $0.30 < p/(M \cdot q) < 0.52$.